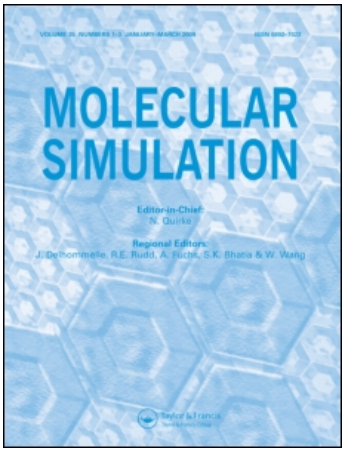

Molecular Simulation
Publication details, including instructions for authors and subscription information:
http://www.informaworld.com/smpp/title~content=t713644482

Simulation Study on Effect of Polymer Entanglement on the Strain Hardening

Yuichi Masubuchi[a]; Jun-Ichi Takimoto[a]; Kiyohito Koyama[a]
[a] Faculty of Engineering, Yamagata University, Yonezawa, Japan

To cite this Article Masubuchi, Yuichi , Takimoto, Jun-Ichi and Koyama, Kiyohito(1999) 'Simulation Study on Effect of Polymer Entanglement on the Strain Hardening', Molecular Simulation, 21: 5, 257 — 269
To link to this Article: DOI: 10.1080/08927029908022068
URL: http://dx.doi.org/10.1080/08927029908022068

Molecular Simulation, 1999, Vol. 21, pp. 257–269
Reprints available directly from the publisher
Photocopying permitted by license only

SIMULATION STUDY ON EFFECT OF POLYMER ENTANGLEMENT ON THE STRAIN HARDENING

YUICHI MASUBUCHI*, JUN-ICHI TAKIMOTO
and KIYOHITO KOYAMA

Faculty of Engineering, Yamagata University, Yonezawa 992-8510, Japan

(Received January 1998; accepted June 1998)

The effect of the molecular entanglement on the elongational viscosity was investigated by Brownian dynamics simulation in 2-dimension. The polymer was represented by freely-rotated bead-rod model. The entanglement constraint was assumed by a repulsive interaction between bonds in the chain and randomly located obstacles. Under an elongational flow, affine deformation was applied to spatial distribution of the obstacles. Varying lifetime and density of the obstacles, we investigated these effect on elongational viscosity. We found that (i) linear viscosity increases with increasing density while it is independent of the lifetime, that (ii) critical strain rate at which the strain hardening begins is independent of both the lifetime and the density, that (iii) the longer lifetime gives the stronger strain hardening, and that (iv) when the density becomes higher than entanglement threshold of the chain, the strain hardening is discontinuously enlarged.

Keywords: Brownian dynamics; polymer rheology; strain hardening; polymer entanglement; elongational flow; elongational viscosity

INTRODUCTION

Since elongational flow is often implicated in polymer processing, the elongational viscosity of polymer melts has been investigated by experiments [1–7] and recently by computer simulations [8, 9]. It has been empirically established that most polymers show strain hardening; the elongational viscosity steeply rises when a strain rate is higher than a certain critical

* Corresponding author. Tel.: 81-238-26-3057, Fax: 81-238-26-3411, e-mail: mas@dip.yz.yamagata-u.ac.jp

value. The mechanism of the strain hardening, however, has not been fully understood.

Recently, Minegishi *et al.* [7] reported that molecular entanglement affects the intensity of the strain hardening. They prepared poly(methylmethacrylate) (PMMA) including a monodispersed ultra high molecular weight (UHMW) component which is ten times larger than matrix polymer, and measured the elongational viscosity for various concentration of the UHMW polymer. They found that (i) when the UHMW polymer is added, strain hardening is observed at a strain rate at which it is not observed for the pure matrix polymer, and that (ii) strain hardening is intensified discontinuously when concentration of the UHMW polymer is larger than entanglement threshold of the UHMW polymer.

To investigate the effect of the entanglement on the strain hardening in more detail, we performed Brownian dynamics simulation for a simple model in which the molecular entanglement is represented by a repulsive interaction between freely rotated chain and randomly arranged obstacles. We discussed effect of the density and the lifetime of the obstacles on the elongational viscosity.

MODEL

Equation of Motion

Figure 1 shows a schematic model of the simulation. A polymer chain was represented by N beads in 2-dimension connected by bonds of constant length a. The position of bead i, $\boldsymbol{r}_i$, obeys following Langevin equation of motion;

$$\zeta \dot{\boldsymbol{r}}_i = -\frac{\partial U^{\text{tot}}}{\partial x_i} + \boldsymbol{f}_i + \zeta \boldsymbol{r}_i \cdot \boldsymbol{v} + \lambda_i \boldsymbol{u}_i - \lambda_{i-1} \boldsymbol{u}_{i-1}, \tag{1}$$

where ζ is friction coefficient, $\boldsymbol{f}_i$ is random force, $\boldsymbol{v}$ is strain rate tensor, λ_i is Lagrange multiplier to keep bond length constant, and $\boldsymbol{u}_i$ is bond vector defined by $\boldsymbol{u}_i = \boldsymbol{r}_{i+1} - \boldsymbol{r}_i$. To fix the bond length, SHAKE algorithm was applied [10]. For integration of the equation of motion, the explicit Euler scheme was applied with a time step of $\Delta t = 1 \times 10^{-3}$.

To apply elongation, we chose $\boldsymbol{v}$ as

$$\boldsymbol{v} = \begin{pmatrix} \dot{\varepsilon} & 0 \\ 0 & -\dot{\varepsilon} \end{pmatrix}, \tag{2}$$

where $\dot{\varepsilon}$ is strain rate.

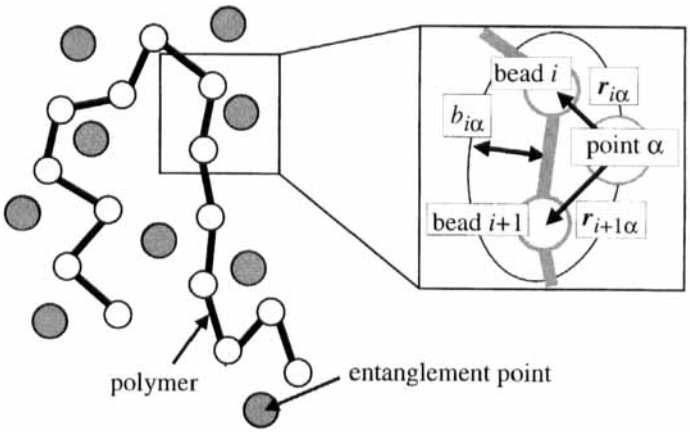

FIGURE 1 Schematic representation of the model. Explanations are in the text.

f_i obeys following Gaussian statistics;

$$\langle f_i \rangle = 0 \tag{3}$$

$$\langle f_i(t) f_j(t') \rangle = 2k_B T \zeta \delta_{ij} \delta(t - t') \boldsymbol{I}, \tag{4}$$

where k_B is Boltzmann constant and T is temperature.

Entanglement Effect

Entanglement Points and Entanglement Potential

In simulation cell, we placed entanglement points where entanglement occurred between the chain and surrounding polymers. To prohibit the chain from passing through the entanglement points, a repulsive interaction was introduced [11, 12]. That is

$$U^{\text{tot}} = \sum_{i}^{\text{bond}} \sum_{\alpha}^{\text{matrix}} U_{i\alpha}^{\text{bond}} + \sum_{i}^{\text{bead}} \sum_{\alpha}^{\text{matrix}} U_{i\alpha}^{\text{bead}} \tag{5}$$

$$U_{i\alpha}^{\text{bond}} = k_B T (\sigma / b_{i\alpha})^6 \tag{6}$$

$$U_{i\alpha}^{\text{bead}} = k_B T (\sigma / |\boldsymbol{r}_{i\alpha}|)^6, \tag{7}$$

where $\boldsymbol{r}_{i\alpha}$ is distance between a bead i and an entanglement point α, and σ is a parameter which determines size of the entanglement point. In this study, σ was set as $U_{i\alpha}^{\text{bead}}(|\boldsymbol{r}_{i\alpha}| = a/4) = k_B T$. $b_{i\alpha}$ is length of shorter axis of an

ellipse which has foci at both ends of a bond i and has curve passing through center of an entanglement point α, and is given by

$$b_{i\alpha} = \frac{1}{2}\left[(|\boldsymbol{r}_{i+1,\alpha}| + |\boldsymbol{r}_{i\alpha}|)^2 - |\boldsymbol{r}_{i\alpha} - \boldsymbol{r}_{i+1,\alpha}|^2\right]^{1/2}, \tag{8}$$

where $\boldsymbol{r}_{i\alpha}$ is a relative vector between a bead i and an entanglement point α (see Fig. 1).

Deformation of the Entanglement Matrix

Initially we randomly distributed the entanglement points of number density C. Assuming that the entanglement points were fixed on the flow, we applied affine deformation to the matrix. Thus, the position of the entanglement point α, $\boldsymbol{s}_\alpha$, was developed as

$$\dot{\boldsymbol{s}}_\alpha = \boldsymbol{s}_\alpha \cdot \boldsymbol{v}. \tag{9}$$

Lifetime of the Entanglement Matrix

To take account molecular weight distribution of the system, we introduced lifetime τ to the entanglement points assuming that the lifetime corresponded to relaxation time of surrounding polymers. To achieve this, we allowed each point to blink with a probability ρ which was related to τ as

$$\rho = \frac{1}{\tau}\Delta t. \tag{10}$$

At every integration step for each point, we generated a random number x, which has an uniform distribution ranging from 0 to 1. When $x < \rho$, the point becomes a "phantom" point which did not interact with the chain but continued to move obeying Eq. (9). For conservation of total number of the entanglement points, another phantom point was randomly selected and it was revived. To do this, we initially prepared randomly distributed phantom points. In this study, the number density of the phantom points C_p was fixed as $C_p = 0.9$.

Simulation Cell

We used periodic boundary condition. Unit cell was deformed by the elongational flow. The calculation was performed till total strain ε became $\varepsilon = 3.0$. To eliminate the size effect of the cell even under such a high strain,

we employed an "oblong" initial cell which was Na to the elongational direction and $21Na$ to the perpendicular direction.

Units and Parameters

We choose the bond length a as the unit length, k_BT as the unit energy, and $\tilde{t} = \zeta a^2/k_BT$ as the unit time. The chain length was fixed as $N = 30$.

To consider an experimental situation in which concentration of UHMW polymer was varied [7], we varied number density of the entanglement points C as 0.01, 0.05, 0.1 and 0.2. Here we assume that the entanglement between the surrounding polymers and the UHMW polymer can be neglected. We can translate C into average pore size of the matrix, ξ, by

$$\xi = C^{-1/2}a - 2\ell, \tag{11}$$

where ℓ is radius of the entanglement points fixed as $\ell = a/4$. According to this, $0.01 \leq C \leq 0.2$ corresponds to $1.7 \leq \xi/a \leq 9.5$. Comparing this with equilibrated size of the chain, $(Na)^{1/2} \simeq 5.5$, and with the bond length, we consider that our simulation includes situations from where UHMW polymer is so sparse that it does not entangle each other, and to where UHMW polymer is so dense that a pure UHMW polymer material is examined.

The life time of the points τ was varied from 10 to 1000 at $C = 0.1$. The examined strain rates $\dot{\varepsilon}$ were from 0.005 to 0.1. We determined them by considering the Rouse relaxation time, τ_R, and the reptation time, τ_d, defined by [13]

$$\tau_R = \frac{\zeta N^2 a^2}{3\pi^2 k_BT} = \frac{N^2}{3\pi^2}\tilde{t}, \tag{12}$$

$$\tau_d = \frac{3Na^2}{\xi^2}\tau_R. \tag{13}$$

Substituting $N = 30$ and $1.7 \leq \xi/a \leq 9.5$, we obtain $\tau_R/\tilde{t} \simeq 30$ and $30 \leq \tau_d/\tilde{t} \leq 950$ for our conditions.

RESULTS AND DISCUSSION

Snapshots

Figures 2 and 3 show typical snapshots. Based on relation between the strain rate and the two characteristic times, the chain behavior in this simulation can be classified into two modes: $1/\tau_R > \dot{\varepsilon} > 1/\tau_d$ and $1/\tau_R < \dot{\varepsilon}$ [4, 13].

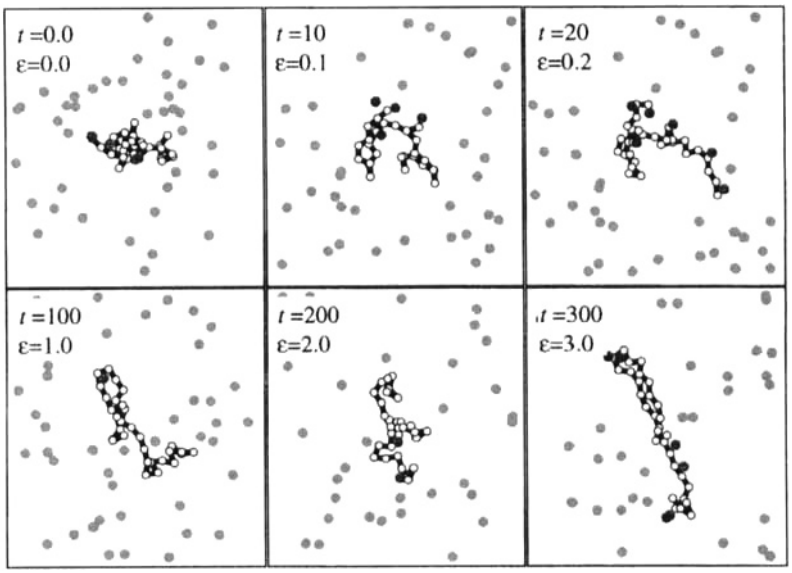

FIGURE 2 Sequential snapshots of a polymer chain and entanglement points under an elongational flow: $N = 30$, $C = 0.1$ and $\dot{\varepsilon} = 0.01$. Time and strain are indicated on each figure.

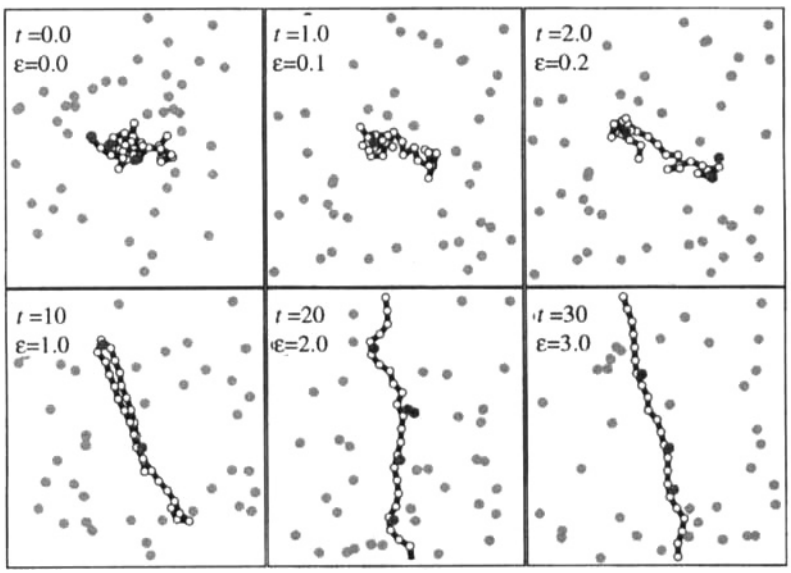

FIGURE 3 Similar to Figure 2 for $\dot{\varepsilon} = 0.1$.

Figure 2 shows the situation of $1/\tau_R > \dot{\varepsilon} > 1/\tau_d$. In this case, speed of the deformation is higher than that of relaxation of the reptation tube. Therefore, the tube is elongated by the flow and thus the chain takes a somewhat elongated conformation. However, speed of the deformation is lower than that of relaxation of the chain in the reptation tube. Thus, each part of the chain is relaxed even when the chain is trapped by the matrix (see $t = 300$ in Fig. 2).

On the other hand, Figure 3 shows the situation of $1/\tau_R < \dot{\varepsilon}$. In this case, the speed of the deformation is higher than both of the speeds of the relaxations: the relaxation of the tube and the relaxation of the chain in the tube. Therefore, the chain is highly stretched.

Calculation of Viscosity

We defined dimensionless elongational viscosity η' by

$$\eta' = \frac{1}{\zeta a^2 N \dot{\varepsilon}} \sum_{i}^{\text{bond}} \lambda_i (-u_{iy}^2 + u_{ix}^2), \tag{14}$$

where $(u_{ix}, u_{iy}) = \boldsymbol{u}_i$. Figures 4 and 5 show time development of η' for various C and τ. In these figures, η' are averaged value for 10 simulations of different initial configurations.

Critical Strain Rate

In Figures 4 and 5, we observe the strain hardening in $\dot{\varepsilon} \geq 0.02$ in all conditions.Thus, a critical strain rate $\dot{\varepsilon}_c$ at which the strain hardening begins exists in $0.02 < \dot{\varepsilon}_c < 0.01$. Though this is somewhat different from the theoretical prediction [4, 13] in which $\dot{\varepsilon}_c = 1/\tau_R \simeq 0.03$, we regard that our model is fair to be discussed.

Linear Viscosity

We regard viscosity for $\dot{\varepsilon} \leq 0.01$ as the linear viscosity, η_l', though η' fluctuates and has different values for $\dot{\varepsilon} = 0.005$ and 0.01. We consider that this is because statistics are not enough. As shown in Figure 4, η_l' becomes larger with larger C. On the other hand, η_l' is not affected by τ (see Fig. 5). This can be explained by the number of the obstacles near the chain. The interaction between the chain and the obstacles generates repulsive force acting on the beads on the chain. This repulsive force also causes an increasing of tension. Thus, the denser matrix gives the higher viscosity.

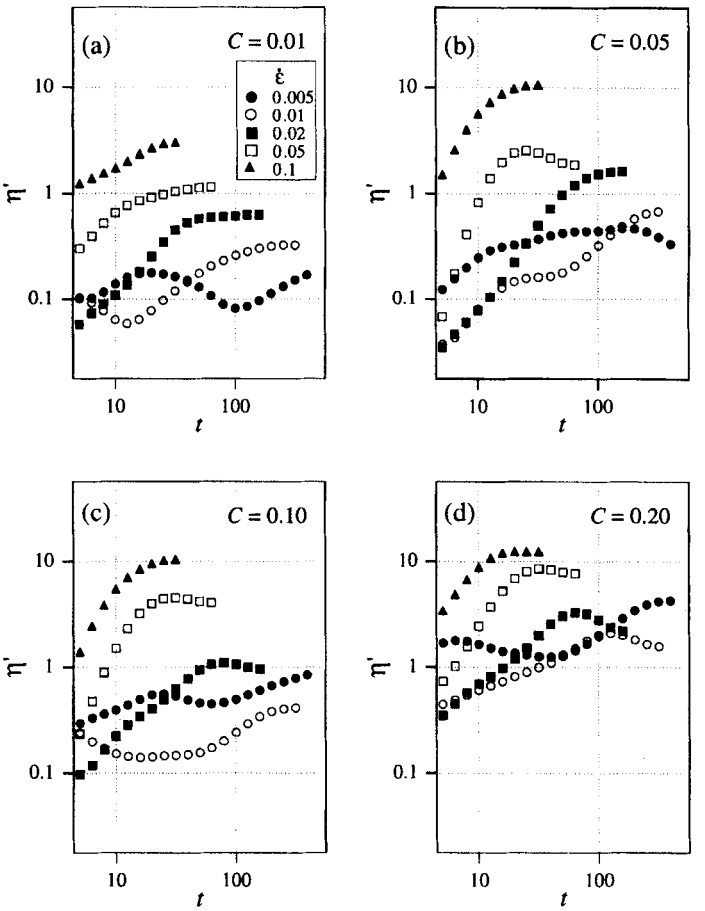

FIGURE 4 Time development of elongational viscosity, η', for various concentration of the entanglement points, C, with various strain rates $\dot{\varepsilon}$. C and $\dot{\varepsilon}$ are indicated on the figures.

The Strain Hardening Properties

Differently from η_l', viscosity for $\dot{\varepsilon} \geq 0.02$ is affected by both C and τ. To investigate the relation in more detail, we calculated the nonlinear parameter [2] ν defined by

$$\nu = \frac{\eta'}{\langle \eta_l' \rangle}, \tag{15}$$

where $\langle \eta_l' \rangle$ is the average of η' for $\dot{\varepsilon} \leq 0.02$. Figure 6 shows ν plotted against strain ε for various $\dot{\varepsilon}$ at $\tau = 1000$. We observe some consistency and

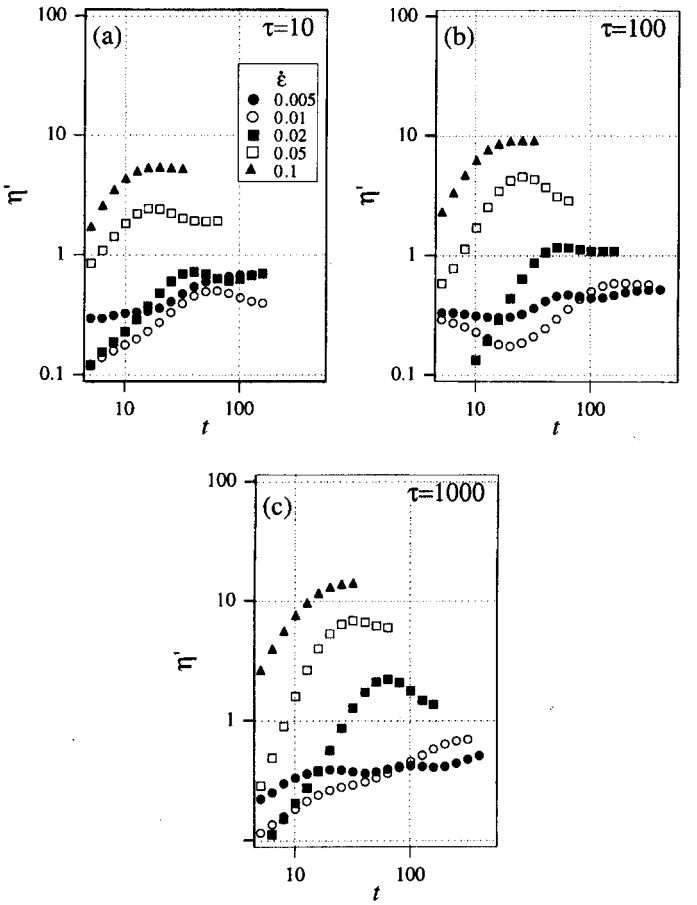

FIGURE 5 Similar to Figure 4 for various lifetime of the entanglement points τ.

inconsistency with the experimental results [2]. It is consistent that (i) the critical strain ε_c where ln ν becomes zero does not depend on $\dot{\varepsilon}$, and that (ii) ln ν linearly increases with increasing ε. On the other hand, it is inconsistent that (i) ε_c is about 0.2 while the most of the experimental results show that it is close to 1, and that (ii) ln ν saturates at a small ε. We conjecture that these are due to the size and the shape of the obstacles representing the entanglement points; the obstacles keep circular shape even under the high strain and limit free space for chain relaxation. It is also considered that the dimension of the simulation and the intra-chain interaction have some effects. The reason is, however, still remained to be discussed.

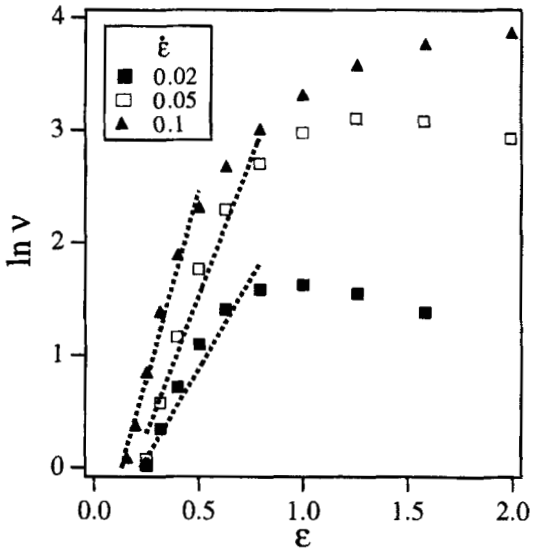

FIGURE 6 Nonlinear parameter, ν, plotted against strain ε for various strain rates $\dot{\varepsilon}$ for $\tau = 1000$. Dotted lines are to guide the eyes.

Assuming that $\ln \nu \propto \varepsilon$, we calculated the intensity of the nonlinearity [2], μ, defined by

$$\mu = \frac{\partial \ln \nu}{\partial \varepsilon}. \tag{16}$$

Figure 7 shows μ as a function of C. We observe that (i) larger $\dot{\varepsilon}$ gives larger μ, that (ii) μ steeply rises for $0.01 < C < 0.05$, and that (iii) μ decreases with increasing C as $\mu \propto C^{-1/3}$ when $C \geq 0.05$ independently of $\dot{\varepsilon}$.

We discuss the rapid increasing of μ for $0.01 < C < 0.05$ by comparing the matrix size with the chain size. Neglecting the intra-chain entanglement, we can estimate entanglement threshold C^* for this system by

$$\xi(C^*) = aN^{1/2}. \tag{17}$$

Combining this with Eq. (11) and substituting $N = 30$, we obtain $C^* \simeq 0.028$. Thus, we consider that μ is enlarged when $C > C^*$. This is consistent with the experimental result by Minegishi *et al.* [7].

Figure 8 shows μ plotted against τ. It is observed that (i) larger $\dot{\varepsilon}$ gives larger μ, that (ii) μ increases with increasing τ roughly described as $\mu \propto \tau^{\gamma}$, and that (iii) μ increases with increasing $\dot{\varepsilon}$. The life time τ can be regarded as

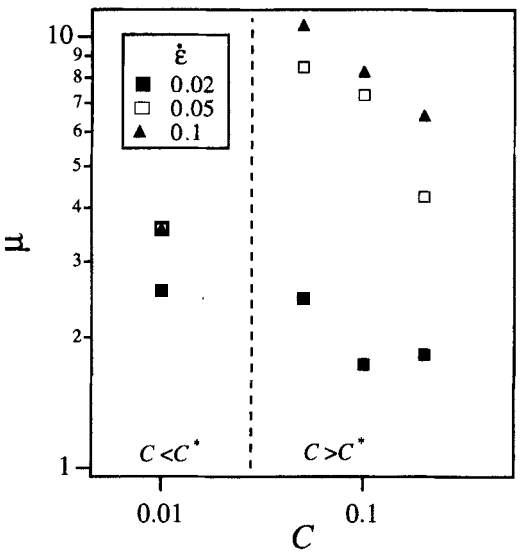

FIGURE 7 Intensity of the nonlinearity, μ, plotted against concentration of the entanglement points C for various strain rates $\dot{\varepsilon}$. Dotted line indicates $C = C^*$.

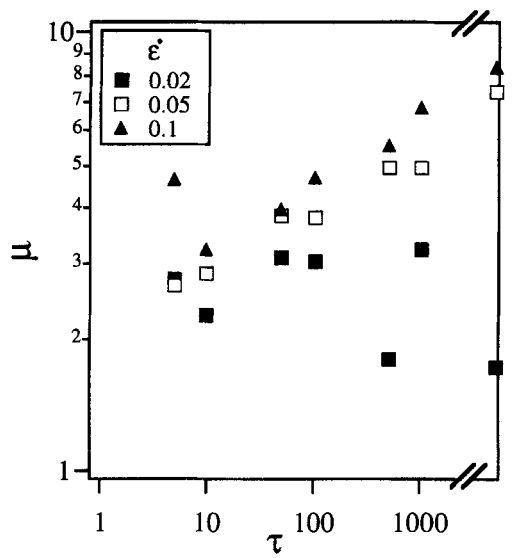

FIGURE 8 Similar to Figure 7 for lifetime of the entanglement points τ. $\tau = \infty$ corresponds to $C = 0.1$ in Figure 7.

the longest relaxation time of the matrix polymers, *i.e.*, their reptation time. Based on this, we can obtain chain length of the matrix N_m as a function of τ by Eqs. (12–11) as

$$N_m = \left[\tau\pi^2\left(C^{-1/2} - \frac{1}{2}\right)^2\right]^{1/3}. \tag{18}$$

Thus, as shown in Figure 8, the shorter the matrix polymers is, the weaker the strain-hardening. When the matrix polymer is very small, it is considered that the matrix does not have any contribution for the strain hardening. This is also consistent with the experimental result [7].

CONCLUSION

We performed simulation of polymer melt using a simple model. Focusing on the strain hardening property of elongational viscosity, we investigated effect of density and lifetime of the entanglement points. We found that (i) linear viscosity increases with increasing density while it is independent of the lifetime, that (ii) critical strain rate at which the strain hardening begins is independent of both the lifetime and the density, that (iii) the larger lifetime gives the stronger strain hardening, and that (iv) when average pore size of the entanglement matrix becomes smaller than $aN^{1/2}$, the strain hardening is enlarged consistently with the experiment by Minegishi *et al.* To support the above results, we have been performing experiments with some polymers which include ultra high molecular weight component. We also have been continuing the calculation to investigate the influence of chain length, branching and distributed lifetime. These results will be concluded and published elsewhere.

Acknowledgement

This work was financially supported in part by Grant-in Aid from the Ministry of Education, Science and Culture, Japan.

References

[1] Meissner, J., Raible, T. and Stephenson, S. E. (1981). "Rotary clamp in uniaxial and biaxial extensional rheometry of polymer melts", *J. Rheol.*, **25**, 1.
[2] Ishizuka, O. and Koyama, K. (1980). "Elongational viscosity at a constant elongational strain rate of polypropylene melt", *Polymer*, **21**, 164.

[3] Münstedt, M. (1980). "Dependence of the elongational behavior of polystyrene melts on molecular weight and molecular weight distribution", *J. Rheol.*, **24**, 847.
[4] Takahashi, M., Isaki, T., Takigawa, T. and Masuda, T.(1993). "Measurement of biaxial and uniaxial extensional flow behavior of polymer melts at constant strain rates", *J. Rheol.*, **37**, 827.
[5] Padmanabhan, M., Kasehagan, L. J. and Macosko, C. (1996). "Transient extensional viscosity from a rotational shear rheometer using fiber-windup technique", *J. Rheol.*, **40**, 473.
[6] Takahashi, T., Wu, W., Toda, H., Takimoto, J., Akatsuka, T. and Koyama, K. (1997). "Elongational viscosity of ABS polymer melts with soft or hard butadiene particles", *J. Non-Newtonian Fluid Mech.*, **68**, 259.
[7] Minegishi, A., Naka, Y., Takahashi, T., Masubuchi, Y., Takimoto, J. and Koyama, K. (1997). "The effect of ultrahigh molecular weight polymers on the nonlinear response in uniaxial elongational viscosity", *J. Soc. Rheol. Jpn.*, **25**, 215.
[8] Kröger, M. and Hess, S. (1996). "Nonequilibrium molecular dynamics computer simulations of polymers", *Proc. XIIth Int. Congr. on Rheology*, p. 321.
[9] Todd, B. D. and Daivis, P. J. (1997). "Elongational viscosities from nonequilibrium molecular dynamics simulations of oscillatory elongational flow", *J. Chem. Phys.*, **107**, 1617.
[10] Allen, M. P. and Tildesley, D. J. (1989). *Computer Simulation of Liquids*, Oxford University Press, Oxford.
[11] Masubuchi, Y., Oana, H., Matsumoto, M., Doi, M. and Yoshikawa, K. (1996). "Conformational dynamics of DNA during biased sinusoidal field gel electrophoresis", *Electrophoresis*, **17**, 1065.
[12] Masubuchi, Y., Oana, H., Matsumoto, M. and Doi, M. (1997). "Brownian dynamics simulation of biased sinusoidal field gel electrophoresis", *Macromolecules*, **30**, 912.
[13] Doi, M. and Edwards, S. F. (1986). *The Theory of Polymer Dynamics*, Oxford University Press, Oxford.